Transport and Transformation of Sulfur compounds over East Asia during the TRACE-P and ACE-Asia Campaigns

Meigen Zhang[1,3], Itsushi Uno[2,3], Yasuhiro Yoshida[4] , Zifa Wang[1,3] and Hajime Akimoto[3]

[1] State Key Laboratory of Atmospheric Boundary Layer Physics and Atmospheric Chemistry, Institute of Atmospheric Physics (IAP), Chinese Academy of Sciences, Beijing 10029, China
[2] Research Institute for Applied Mechanics, Kyushu University, Kasuga Park 6-1, Kasuga 816-8580, Japan
[3] Frontier Research System for Global Change, Yokohama 236-0061, Japan
[4] Graduate School of Engineering Science, Kyushu University, Kasuga Park 6-1, Kasuga 816-8580, Japan

Abstract. On the basis of recently estimated emission inventory for East Asia with a resolution of 1^{o}x1^{o}, the transport and chemical transformation of sulfur compounds over East Asia during the period of February 22 through May 4, 2001, was investigated by using the Models-3 Community Multi-scale Air Quality (CMAQ) modeling system with meteorological fields calculated by the Regional Atmospheric Modeling System (RAMS). For evaluating the model performance simulated concentrations of sulfur dioxide (SO_2) and aerosol sulfate (SO_4^{2-}) were compared with the observations on the ground level at four remote sites in Japan and on board of aircraft and vessel during TRACE-P (the Transport and Chemical Evolution over the Pacific) and ACE-Asia (Asian Pacific Regional Aerosol Characterization Experiment) field campaigns, and it was found that the model reproduces many of the important features in the observations, including horizontal and vertical gradients. The SO_2 and SO_4^{2-} concentrations show pronounced variations in time and space, with SO_2 and SO_4^{2-} behaving differently due to the interplay of chemical conversion, removal and transport processes. Analysis of model results shows that emission was the dominant term in regulating the SO_2 spatial distribution, while conversion of SO_2 to SO_4^{2-} in the gas phase and the aqueous phase and wet removal were the primary factors that control SO_4^{2-} amounts. The gas phase and the aqueous phase have the same importance in oxidizing SO_2, and about 42%

sulfur compounds (~25% in SO_2) emitted in the model domain was transported out, while about 57% (~35% by wet removal processes) deposited in the domain during the study period.

Key words: Long-range transport, SO_2, Sulfate, ACE-Asia, Chemical Transport Model

Corresponding Author: Meigen Zhang, State Key Laboratory of Atmospheric Boundary Layer Physics and Atmospheric Chemistry, Institute of Atmospheric Physics (IAP), Chinese Academy of Sciences, Beijing 10029, China. E-mail: mgzhang@mail.iap.ac.cn, Fax:86-10-62041393

Submitted for ASAAQ special issue of *Atmospheric Environment* on April 30, 2003.

1. Introduction

Sulfur dioxide (SO_2) is one of the most important individual precursor compound for secondary matter in the atmosphere. Aerosol sulfate (SO_4^{2-}) has been identified as an important contributor to the scatter of sunlight, and a major component of cloud condensation nuclei [*Lelieveld and Heintzenberg,* 1992; *Chuang et al.,* 1997]. In addition to these, sulfate is an important acidifying agent and a potential cause of adverse health effects observed in urban areas [*Rodhe*, 1999]. Sulfur compounds are especially important in East Asia in view of the fact that pollutant emission has been continuously and rapidly increasing over the last decades [e.g., *Streets et al.*, 2000] and is expected to continue to increase for the coming ones, e.g., SO_2 emissions in China are projected to increase from 25.2 mt (million ton) in 1995 to 30.6 mt in 2020, provided emission controls are implemented on major power plants [*Streets and Waldhoff*, 2000], and they can be transported long distance up to several thousand kilometers.

SO_4^{2-} is primarily produced from the oxidation of SO_2, and the conversion of SO_2 to SO_4^{2-} occurs via multiple pathways, including gas phase oxidation to sulfuric acid (H_2SO_4) followed by condensation into the particulate phase, aqueous phase oxidation in cloud or fog droplets, and various reactions on the surfaces or inside aerosol particles. In the last two decades a variety of transport and acid deposition models have been developed or applied to address sulfur transport, transformation and deposition over East Asia [e.g., *Huang, et al., 1995; Ichikawa et al., 1997; Xiao et al., 1997; Xu and Carmichael, 1999; Murano et al., 2000; Qian et al., 2001;Kim, et al., 2001*]. This study is another attempt to investigate the

behavior of SO_2 and SO_4^{2-} over East Asia at range of temporal and spatial scales, and to examine the relative role of emission, meteorological fields, chemical and removal mechanisms in regulating this behavior with a comprehensive chemical transport model on the basis of newly estimated emission inventory for East Asia with a resolution of $1^o x 1^o$ prepared specially to support the Transport and Chemical Evolution over the Pacific (TRACE-P; *Jacob et al., 2003*) and the Asian Pacific Regional Aerosol Characterization Experiment; (ACE-Asia; *Huebert et al., 2003*) and large observational datasets obtained at four remote sites as an East Asia Acid Rain Monitoring Network (EANET) in Japan and on board of aircraft and ship during TRACE-P and ACE-Asia field campaigns.

In section 2 we briefly describe the model, its initial and boundary conditions, and emission inventories, and in section 3 we firstly compare modeled SO_2 and SO_4^{2-} mixing ratios with observations and discuss their temporal and spatial concentration distributions, and then examine the relative importance of different physical and chemical processes in determining SO_2 and SO_4^{2-} concentrations. Conclusion is given in Section 4.

2. Model Descriptions

The transport and chemical evolution of sulfur compounds over East Asia is investigated by use of the Models-3 Community Multi-scale Air Quality (CMAQ) modeling system [*Byun and Ching*, 1999]. CMAQ is an Eulerian-type model developed in the U.S. Environmental Protection Agency to address tropospheric ozone, acid deposition, visibility, particulate matter and other pollutant issues in the context of "one atmosphere" perspective where complex interactions between atmospheric pollutants and regional and urban scales are confronted. CMAQ has recently been successfully applied to East Asia to simulate tropospheric ozone [*Zhang et al.,* 2002, 2003].

The current version of the model is configured with the chemical mechanism of the Regional Acid Deposition version 2 [RADM2; *Stockwell et al.*, 1990], having been extended to include the four-product Carter isoprene mechanism [*Carter*, 1996] and aerosol processes from direct emissions and production from sulfur dioxide, long-chain alkanes, alkyl-substituted benzene, etc. To depict aerosol evolution processes in the atmosphere, the aerosol module, a major extension of the Regional Particulate Model [RPM; *Binkowski and Shankar*, 1995] is included. In the module the particle size distribution is represented as the superposition of three lognormal sub-distributions, and the processes of coagulation, particle growth by the addition of new mass, particle formation, dry deposition, cloud processing,

aerosol chemistry, etc. are included. The complete mechanisms with lists of species and reactions in the model are described in detail by *Byun and Ching* [1999].

For CMAQ, the anthropogenic emissions of nitrogen oxides, carbon monoxide, volatile organic compounds (VOCs) and SO_2 were obtained from the emission inventory of 1^ox1^o specially prepared by scientists at the Center for Global and Regional Environmental Research at the University of Iowa [*Streets et al.,* 2002] to support TRACE-P and ACE-Asia and from the Emission Database for Global Atmospheric Research [EDGAR; *Oliver et al.,* 1996]. NO_x emissions from soils and natural hydrocarbon emissions were obtained from the Global Emissions Inventory Activity (GEIA) 1°x1° monthly global inventory [*Benkovitz et al.,* 1996] for the month of March. VOC emissions were apportioned appropriately among the lumped-hydrocarbon categories used in RADM2. Natural sources consist of the active volcanic sources in the region. The emissions from the largest erupting volcano of Miyakejima, located to the south of Tokyo, were updated based on the flux measurements (http://staff.aist.go.jp/kazahaya-k/miyakegas/COSPEC.html). The SO_2 emissions from this volcano eruption contributed two third of total SO_2 emitted over Japan. In this study it is assumed that 5% SO_2 emitted was in the form of H_2SO_4.

The three dimensional meteorological fields needed by CMAQ are provided by the Regional Atmospheric Modeling System [RAMS; *Pielke et al.,* 1992]. In this study RAMS is excised in a four-dimensional data assimilation mode using analysis nudging with re-initialization every four days, leaving first 24 hours as initialization period. The three-dimensional meteorological fields for RAMS were obtained from the European Center for Medium-Range Weather Forecasts (ECMWF) analyzed datasets, and were available every six hours with 1°□1° resolution. Besides, Sea Surface Temperatures (SST) for RAMS were based on weekly mean values and observed monthly snow-cover information as the boundary conditions for the RAMS calculation.

The study domain (shown in Figure 1) is 6240x5440 km^2 on a rotated polar-stereographic map projection centered at (25^oN, 115^oE) with 80 km grid cell. For RAMS there are 23 vertical layers in the σ_z coordinates system unequally spaced from the ground to ~23 km, with about 9 layers concentrated in the lowest 2 km of the atmosphere in order to resolve the planetary boundary layer, while there are 14 levels for CMAQ with the lowest 7 layers being the same as those in RAMS.

Initial and boundary conditions of species were chosen to reflect the East Asian situation. Recent measurements were used whenever possible [*Zhang et al*., 2003]. To evaluate the

impact of the anthropogenic emissions on the distributions of trace gases and aerosols, the initial and boundary conditions were generally chosen at the lower end of their observed range (e.g., the northern and western boundary conditions for SO_2 and SO_4^{2-} were 0.3 ppbv and 1 $\mu g/m^3$, respectively) so as to allow the emissions and chemical reactions to bring them closer to their actual values during the initialization period [*Liu et al.,* 1996; *Carmichael et al.,* 1998].

In order to trace the volcano plume behavior, we also used the Lagrangian particle model (RAMS/HYPACT; Hybrid particle and concentration transport model; *Walko et al*, 2001). RAMS calculated meteorological results were used in HYAPCT dispersion calculation, and the constant particle emission is assumed over the Miyakejima volcano. HYPACT particle field will be discussed with CMAQ SO_2 and SO_4^{2-} concentration field.

3. Model Results and Discussion

The simulation period covers February 22 to May 5, 2001 with starting time at 0000 Z on February 22, i.e., 0900 JST (Japanese Standard Time), when the TRACE-P and the ACE-Asia missions were being conducted over the Western Pacific Ocean, which provides extensive observational data to evaluate the model performance and further to quantify the spatial and vertical distribution of SO_2 and SO_4^{2-}, the processes controlling their formation, evolution and fate.

3.1 Transport and Chemical Evolution of SO_2 and SO_4^{2-} in the boundary layer

The meteorological situation is genuinely central to the distribution of many atmospheric chemical species [*Merrill et al.,* 1997]. This is because meteorological parameters impact both the chemical processes and the transport phenomena, which govern the evolution of these distributions. Comparison of the meteorological parameters (such as wind speed and direction, temperature and water mixing ratio) simulated by RAMS with airborne measurements on board of NASA aircraft DC-8 and P-3B [*Jacob et al.*, 2003] and NCAR aircraft C-130 [*Huebert et al.*, 2003] showed that the modeled meteorology reproduced quantitatively most of the major observed features [*Uno et al.,* 2003]. For example the correlation coefficients for wind speed, temperature and relative humidity each exceeded 0.9 for all TRACE-P observation points for altitudes below ~5 km.

Spring is the season of maximum Asian outflow over the Pacific due to a combination of

active convection over the continent and strong westerlies, and the intermittent SO_2 peaks observed at four remote sites in Japan shown in Figure 2. It shows the time variations of hourly averaged SO_2 concentrations measured at the sites (EANET) of Hedo (Fig. 2a), Oki (Fig. 2b), Happo (Fig. 2c), and Sado (Fig. 2d). Also shown are the results from the model for the lowest model layer, approximately 75 m above the ground. The locations of the observation sites are shown in Figure 1. Figure 2 suggests that Asian outflow is highly episodic [*Yienger et al.,* 2000].

From Figure 2 we can see that the model captures the time variation of SO_2 mixing ratios in the simulation period very well, and in most cases simulated and observed concentrations are in good agreement, for example, the magnitude and timing of the peak SO_2 levels around Julian Day (JD) 100 (i.e., April 10) at all four sites were well captured, while some simulated SO_2 spikes at Hedo around JD 78 (i.e., March 19) and 116 (i.e., March 26) are not well seen in observations, and some observed elevated values at four sites are not reproduced in simulations (e.g., JD 110 at Sado). As SO_2 is mostly emitted in the continental boundary layer, and its concentrations at these remote sites are primarily dependent on transport processes, so the good agreement between simulated and observed SO_2 mixing ratios implies that the SO_2 emissions, wind fields and transport processes were reasonably well treated in the RAMS and CMAQ model.

During the ACE-Asia mission, NOAA Research Vessel Ronald H. Brown (RonBrown) made continuous observations around Japan. Its ship track and observed concentrations of SO_2 and SO_4^{2-} are presented in Figure 3. Also shown in the figure are simulated hourly averaged concentrations sampled along the ship track. Figure 3 shows high SO_2 mixing ratios (up to 35 ppbv) over the area south to Tokyo around JD 90 (i.e., March 31) and 109 (i.e., April 19) and over the Sea of Japan around JD 100 (i.e., April 10), and high SO_4^{2-} mixing ratios over Sea of Japan around JD 100 (April 10). High SO_2 and low SO_4^{2-} concentrations over the area south to Tokyo clearly shows the area was under strong influence of fresh SO_2 plume from the Miyakejima volcano, and the model reproduces this observed feature quite well. High SO_2 and SO_4^{2-} concentrations over the Sea of Japan are also captured by the model and are identified to be associated with the emissions from the Miyakejima volcano (see Figure 5 and 6). From the figure we find that the model overestimates both SO_2 and SO_4^{2-} concentrations around JD 100 (i.e., April 10) and SO_2 concentrations around JD 109 (i.e., April 19), while underestimates SO_2 concentrations around April 89 (i.e., March 30). This discrepancy in elevated SO_2 and SO_4^{2-} values between observations and simulations are

primarily caused by the constant setting of the volcano emission rate, which was assumed time invariant in the model but in fact volcano activity varied significantly with time (or day by day).

In Figures 4 and 5 we will show horizontal distributions of SO_2 and SO_4^{2-} concentrations and wind vectors for the lowest model layer (approximately 150 m) at 1200 JST during April 9 to 13, when elevated SO_2 and SO_4^{2-} concentrations were observed at all the four measurement sites and over the Sea of Japan. In Figure 6, we also show the vertically averaged SO_2 concentration field from HYAPCT particle model. It should be noted that Figure 6 only shows the contribution from Miyakejima volcano to understand the impact of volcano emission.

Figure 4a clearly shows a low-pressure in the Okinawa area of Japan, one weak high-pressure in northeastern China and another high-pressure located to the east of Japan. High SO_2 concentrations are seen in the source regions, e.g., Sichuan Province, Shanghai and Beijing areas in China, Seoul and Pusan areas in Korea and the Miyakejima area just south of Tokyo, Japan. High SO_2 values over the Sea of Japan were associated with the Miyakejima volcano emissions (see Figure 6a), which is clearly shown in the figure. From Figures 2b, 2c, 2d and 3b we can see elevated SO_2 values at Oki, Happo, Sado and over the Sea of Japan at this time. The SO_2 dispersion calculation results shown in Figure 6 clearly shows the impact of Miyakejima volcano reached to the western part of Japan area and it has a good agreement with surface SO_2 peak.

The horizontal distributions of SO_4^{2-} mixing ratios shown in Figure 5a is generally consistent with these of SO_2 where its mixing ratios are high, i.e., elevated SO_4^{2-} concentrations are also seen in Sichuan Province, Shanghai and Beijing areas in China, Seoul and Pusan areas in South Korea and over the Sea of Japan. Obvious differences between Figures 4a and 5a are seen over the western Pacific and the inner Asian continent covering northwestern China and Mongolia. Over the western Pacific we see SO_2 levels are lower than 0.1 ppbv while SO_4^{2-} values are higher than 1 $\mu g/m^3$. In contrast, over the inner Asian continent SO_2 levels are higher than 0.1 ppbv while SO_4^{2-} values are lower than 1 $\mu g/m^3$. These differences are primarily associated with different weather and chemical conditions and are seen in the next 3 days. As temperature and water contents in the surface air over the western Pacific are higher than over the inner Asian continent, and concentrations of hydroxyl radical (OH) and hydrogen peroxide (H_2O_2) are also higher, so SO_2 is oxidized faster via the gas-phase and the aqueous-phase over the western Pacific than over the inner Asian continent,

and coordinately SO_4^{2-} concentrations are higher over the western Pacific as it is primarily produced from the oxidation of SO_2. Besides, high SO_4^{2-} concentrations over the western Pacific maybe partially attribute to its direct transport from the continent.

On April 10 and 11 (i.e., JD 100 and 101) the central and eastern China was under influence of a high pressure located in northwestern China and the low-pressure moved eastward from the Okinawa area. We see in Figures 4b, 4c, 5b and 5c that over southern Japan and the area to the south of Japan, strong northeast winds sweep SO_2 and SO_4^{2-} to East China Sea and Okinawa area, while anticyclonic circulation over the Asian continent pushes pollutants within the continent out to sea, then brings them southward.

Figures 4b and 6b indicate Oki is experiencing high SO_2 levels associated with the volcano plume, and the observations recorded the highest SO_2 concentrations at Oki (Figure 2b). On April 10 high SO_2 values appeared at Happo (Figure 2c) and on the next day at Hedo (Figure 2a).

On April 12 (i.e., JD 102) a traveling cold front swept across the continent, and moved eastward. Figures 4d and 5d clearly show strong continental outflow from eastern and northeastern China and Korea associated with the front. In Figure 5d we find a belt of elevated SO_4^{2-} concentrations in the fore part of the front, where high water contents and cloud processes associated with frontal uplifting lead to increase in SO_4^{2-} production, and low SO_4^{2-} concentrations in the back part the front due to the subsidence of cool, dry and SO_4^{2-} poor air, even SO_2 mixing ratios are high (>2 ppbv) there (Figure 4d). High SO_2 values were recorded at Hedo in the next several days (Figure 2a).

In this section we find that the model reproduces the observed variations of SO_2 and SO_4^{2-} concentrations well, and in most cases simulated and observed values are in good agreement. Analysis of model results shows that the Miyakejima volcano emissions have strong influence upon SO_2 and SO_4^{2-} levels around Japan, and the SO_2 and SO_4^{2-} concentrations exhibit pronounced variations in time and space, with SO_2 and SO_4^{2-} behaving differently due to the interplay of chemical conversion, removal and transport processes.

3.2 Vertical concentration distributions of SO_2 and SO_4^{2-} along the flight tracks

During the ACE-Asia missions, instrumented NCAR aircraft C-130 conducted extensive flights over Yellow Sea, the Sea of Japan and south of Japan, and here we present three typical flights to show vertical distributions of SO_2 and SO_4^{2-} concentrations over these areas. Figures 7, 8 and 9 show C130 flight tracks conducted in the period of April 11-13 and time series of

observed and simulated SO_2 and SO_4^{2-} concentrations along the flight tracks. In these figures the observed SO_2 and SO_4^{2-} concentrations were 5-minute averaged, while the model results were sampled along the flight tracks with a 1-hour temporal resolution.

On April 11(RF06) and 12 (RF07), C-130 made extensive observations over the Yellow Sea. It took off at about 0900 JST from the Marine Corps Air Station Iwakuni, located on the west side of main island of Honshu, Japan, and firstly headed westward and then northward (Figure 7a and 8a). The measured SO_2 and SO_4^{2-} concentrations (Figures 7b, 7c, 8b, and 8c) exhibit large variations in time and space and show high values and good correlation between them in the lower troposphere (below 2 km), as SO_2 is mostly emitted in the continental boundary layer and SO_2 and SO_4^{2-} levels over the Yellow Sea depend primarily on transport processes of SO_2 and SO_4^{2-} and chemical conversion of SO_2 to SO_4^{2-}. At an altitude above 2 km, SO_2 mixing ratios were quite low, and SO_2 and SO_4^{2-} do not show any correlation, which may be due to the depletion of SO_2.

On April 13 (RF08), C-130 started observations at about 0900 JST, and firstly flew northeastward and then southwestward (Figure 9a). SO_2 levels measured during the flight were lower over the Yellow Sea than that obtained in previous flights, while SO_4^{2-} levels were higher, as part of SO_2 was converted to SO_4^{2-} during transport processes (see Figures 4 and 5). It is important to point out that the modeled SO_4^{2-} is underestimated (about 2-3 ug/m^3) during the time between 1230 and 1530JST when the C-130 fly over the east edge of East China sea (Figure 9a). However, we can see the high SO_4^{2-} region is just west of flight area (Figure 5e), so the reason of this under estimation can be understood as model horizontal resolution.

From Figures 7, 8 and 9 we find that the modeled and observed SO_2 to SO_4^{2-} concentrations are generally in good agreement, and the model reproduces time and space variations in SO_2 to SO_4^{2-} reasonably well.

3.3 Process Analysis for Sulfur Compounds

SO_4^{2-} is primarily produced from the oxidation of SO_2, and the conversion of SO_2 to SO_4^{2-} occurs via multiple pathways, including gas phase oxidation to H_2SO_4 followed by condensation into the particulate phase, aqueous phase oxidation in cloud or fog droplets, and various reactions on the surfaces or inside aerosol particles. For illustrating the impacts of the emissions, as well as various transport and chemical processes, upon SO_2 and SO_4^{2-} concentrations, a processes analysis was performed. In Table 1 the sources and sinks of SO_2, H_2SO_4 and SO_4^{2-} in the whole model domain below 16 km in the period from March 1 to

April 30 of 2001 are summarized. In the table TRT includes the contributions from transport and diffusion processes, CHEM stands for the gas-phase chemical production, AQUE accounts for the impacts of aqueous chemistry and cloud processes, G2P represent SO_4^{2-} production via the gas to particle process, EMIS stands for emissions, and DRY and WET are for dry and wet deposition. Negative values indicate the mass of the species decreased by this processes.

In Table 1, the budgets for SO_2 and SO_4^{2-} clearly summarize the conversion pathway of SO_2 to SO_4^{2-} in the study period. The SO_2 budget shows that ~49% (the sum of AQUE and CHEM divided by EMIS) SO_2 emitted is oxidized to SO_4^{2-}, ~25% deposited by dry and wet removal processes, and ~26% transported out of the domain. CHEM and AQUE have the same importance in oxidizing SO_2 (AQUE contributes ~68%), and dry deposition is more important than wet deposition in removing SO_2.

From the SO_4^{2-} budget, we see that the aqueous-phase conversion of SO_2 to SO_4^{2-} contributes more than 61% (AQUE divided by the sum of AQUE and G2P) to the total SO_4^{2-} production, ~35% (TRT divided by the sum of AQUE and CHEM) of SO_4^{2-} is transported out of the domain, and ~63% of SO_4^{2-} is removed by wet deposition, while ~2% by dry deposition.

From Table 1 we find that ~42% (total TRT divided by total EMIS) sulfur compounds (~26% in SO_2) emitted in the domain was transported out, while ~57% (~32% by wet removal processes) deposited in the domain. It is worthy to note that more SO_2 than SO_4^{2-} transported out of the domain was associated with Miyakejima volcano emissions, as the volcano is located near the east downwind boundary, so its SO_2 emission was directly transported out before converted to SO_4^{2-}.

4. Conclusions

The Models-3 Community Multi-scale Air Quality (CMAQ) modeling system with meteorological fields calculated by the Regional Atmospheric Modeling System (RAMS) was applied to East Asia to investigate the transport and chemical transformation processes of SO_2 in the springtime of 2001. Comparison of simulated concentrations of SO_2 and SO_4^{2-} with surface observations at four remote sites in Japan and airborne and ship measurements during TRACE-P and ACE-Asia indicates that CMAQ reproduces many of the important features in the observations, including horizontal and vertical gradients. The SO_2 and SO_4^{2-} concentrations show pronounced variations in time and space, with SO_2 and SO_4^{2-} behaving

differently due to the interplay of chemical conversion, removal and transport processes.

Analysis of model results shows that emission is the dominant term in regulating the SO_2 spatial distribution, while conversion of SO_2 to SO_4^{2-} in the gas phase and the aqueous phase and wet removal processes are the primary factors that control SO_4^{2-} amounts. The emissions from the Miyakejima volcano played a very important role in forming high levels of SO_2 and SO_4^{2-} around Japan as recorded at the four remote sites of Oki, Happo, Sado, and Hedo and aboard of Ship RonBrown in the period April 9-13.

Analysis of sulfur budgets in the period March 1 to April 30 indicates that the gas phase and the aqueous phase have the same importance in oxidizing SO_2 (~68% via the aqueous phase) in the model domain, and about 42% sulfur compounds (~25% in SO_2) emitted in the domain is transported out of the model domain, while about 57% (~35% by wet removal processes) deposited in the domain.

Acknowledgements

This work was partly supported by Research and Development Applying Advanced Computational Science and Technology (ACT-JST), Core Research for Evolution Science and Technology (CREST) of Japan Science and Technology Corporation (JST), National Natural Science Foundation of China (project number: 40245029), and Hundred Talents Program (Global Environmental Change) of Chinese Academy of Sciences. The authors want to express their special thanks to Dr. Alan Bandy and Dr. Byron Blomquist for C-130 SO_2 measurement, Dr. Barry Huebert for C-130 SO_4^{2-} measurement and to Dr. Jim Johnson for RonBrown SO_2 measurement. EANET SO_2 observation data were provided from the Acid Deposition and Oxidant Research Center, Niigata, Japan.

This research is a contribution to the International Global Atmospheric Chemistry (IGAC) Core Project of the International Geosphere Biosphere Program (IGBP) and is part of the IGAC Aerosol Characterization Experiments (ACE).

References

Benkovitz, C.M., M.T. Schultz, J. Pacyna, L. Tarrason, J. Dignon, E.C. Voldner, P.A. Spiro, J.A. Logan, and T.E. Graedel, Global gridded inventories of anthropogenic emissions of sulfur and nitrogen, *J. Geophys. Res.,* **101**, 29239-29253, 1996.

Binkowski, F.S., and U. Shankar, The regional particulate matter model: 1. Model description and preliminary results, *J. Geophys. Res.,* **100**, 26,191-26,209, 1995.

Byun, D.W., and J.K.S. Ching, ed., *Science algorithms of the EPA Models-3 community multi-scale air quality (CMAQ) modeling system*, NERL, Research Triangle Park, NC, 1999.

Carmichael, G.R., I. Uno, M.J. Phadnis, Y. Zhang, and Y. Sunwoo, Tropospheric ozone production and transport in the springtime in east Asia, *J. Geophys. Res.,* **103**, 10,649-10,671, 1998.

Carter, W.P.L., Condensed atmospheric photooxidation mechanisms for isoprene, *Atmos. Environ.,* **24**, 4,275-4,290, 1996.

Chuang, C.C., J.E. Penner, K.E. Taylor, A.S. Grossman, and J.J. Walton, An assessment of the radiative effects of anthropogenic sulfate, *J. Geophys. Res.,* **102**, 3761-3778, 1997.

Huang, M., Z. Wang, D. He, H. Xu, and L. Zhou, Modeling studies on sulfur deposition and transport in East Asia, *Water Air Soil Pollut.,* **85**, 1927-1932, 1995.

Huebert, B., T. Bates, P. Russell, G. Shi, Y.J. Kim, and K. Kawamura, An overview of ACE-Asia: strategies for quantifying the relationships between Asian aerosols and their climatic impacts, to be submitted *J. Geophys. Res.* 2003.

Ichikawa, Y., H. Hayami, and S. Fujita, A long-range transport model for East Asia to estimate sulfur deposition in Japan, *J. Applied Meteorology,* **37**, 1364-1374, 1998.

Jacob, D. J., J. H. Crawford, M. M. Kleb, V. E. Connors, R. J. Bendura, J. L. Raper, G. W. Sachse, J. C. Gille and L. Emmons, The Transport and chemical evolution over the Pacific (TRACE-P) Mission: Design, execution, and overview of first results. *J. Geophys. Res.* 2003. (in press)

Kim, B.-G., J.-S. Han, and S.-U. Park, Transport of SO_2 and aerosol over the Yellow sea, *Atmos. Environ.,* **35**, 727-737, 2001.

Lelieveld, J., and J. Heintzenberg, Sulfate cooling effect on climate through in-cloud oxidation of anthropogenic SO_2, *Science*, **258**, 117-120, 1992.

Liu, S.C., et al., Model study of tropospheric trace species distributions during PEM-West A, *J. Geophys. Res.,* **101**, 2073-2085, 1996.

Merrill, J.T., R.E. Newell, and A.S. Bachmeier, A meteorological overview for the Pacific Exploratory Mission-West, Phase B, *J. Geophys. Res.,* **102**, 28,241-28,253, 1997.

Murano, K., H. Mukai, S. Hatakeyama, E.S. Jang, and I. Uno, Trans-boundary air pollution over

remote islands in Japan: observed data and estimates from a numerical model, *Atmos. Environ.,* **34**, 5139-5149, 2000.

Oliver, J.G.J., et al., Description of EDGAR Version 2.0: *A set of global emission inventories of greenhouse gases and ozone-depleting substances for all anthropogenic and most natural sources on a per country basis and on 1^0x1^0 grid,* National Institute of Public Health and the Environment (RIVM) report no. 771060 002 / TNO-MEP report no. R96/119, 1996.

Pielke, R.A., W.R. Cotton, R.L. Walko, C.J. Tremback, W.A. Lyons, L.D. Grasso, M.E. Nicholls, M.D. Moran, D.A. Wesley, T.J. Lee and J.H. Copeland, A comprehensive meteorological modeling system – RAMS, *Meteorol. Atmos. Phys.*, 49, 69-91, 1992.

Qian, Y., F. Giorgi, Y. Huang, W. Chameides, and C. Luo, Regional simulation of anthropogenic sulfur over East Asia and its sensitivity to model parameters, *Tellus*, **53B**, 171-191, 2001.

Rodhe, H., Human impact on the atmospheric sulfur balance, *Tellus*, **51A-B**, 110-122, 1999.

Stockwell, W.R., P. Middleton, J.S. Chang, and X. Tang, The second generation regional acid deposition model chemical mechanism for regional air quality modeling, *J. Geophys. Res.,* **95**, 16,343-16,367, 1990.

Streets, D.G., and S.T. Waldhoff, Present and future emissions of air pollutants in China: SO_2, NO_x and CO, *Atmos. Emviron.*, **34**, 363-374, 2000.

Streets, D.G., N.Y. Tsai, H. Akimoto, and K. Oka, Sulfur dioxide emissions in the period 1985-1997, *Atmos. Environ.,* **34**, 4413-4424, 2000.

Streets, D.G., T.C. Bond, G.R. Carmichael, S. Fermandes, Q. Fu, D. He, Z. Klimont, S. M. Nelson, N.Y. Tsai, M.Q. Wang, J.-H. Woo, and K.F. Yarber, A inventory of gaseous and primary aerosol emissions in Asia in the year 2000, *J. Geophys. Res.*, 2002. (submitted)

Uno, I., G.R. Carmichael, D. Streets, Y. Tang et.al. ; Regional Chemical Weather Forecasting System CFORS: Model Description and Analysis of Surface Observations at Japanese Island Stations During the ACE-Asia Experiment, *J. Geophy. Res.*, 2003. (in press)

Walko,R.L., Tremback, C.J. and Bell,M.J.: HYPACT Hybird Particle And Concentration Transport Model User's Guide, Mission Research Corp., August 2001.

Xiao, H., G.R. Carmichael, J. Durchenwald, D. Thornton, and A. Bandy, Long-range transport of SOx and dust in East Asia during the PEM B experiment, *J. Geophys. Res.,* **102**, 28,589-28,612, 1997.

Xu, Y., and G.R. Carmichael, An assessment of sulfur deposition pathways in Asia, *Atmos. Environ.,* **33**, 3473-3486, 1999.

Yienger, J.J., M. Galanter, T.A. Holloway, M.J. Phadnis, S.H. Guttikunda, G.R. Carmichael, W.J.

Moxim, and H. Levy II, The episodic nature of air pollution transport from Asia to North America, *J. Geophys. Res.*, **105**, 26,931-26,945, 2000.

Zhang, M., I. Uno, S. Sugata, Z. Wang, D. Byun, and H. Akimoto, Numerical study of boundary layer ozone transport and photochemical production in east Asia in the wintertime, *Geophys. Res. Lett.*, 10.1029/2001GL014368, 2002.

Zhang, M., I. Uno, Z. Wang, H. Akimoto, G.R. Carmichael, Y. Tang, J.H. Woo and others; Large-scale Structure of trace gas and aerosols distributions over the western Pacific Ocean during the TRACE-P, *J. Geophys. Res. 2003*. (in press)

Table 1. Sources and sinks of SO_2, H_2SO_4 and SO_4^{2-} in the whole model domain below 16km (6240×5440×16 km^3) in the period March 1 to April 30 of 2001 (Unit: 10^{10}gS)

	TRT	CHEM	AQUE	G2P	EMIS	DRY	WET
SO_2	-2.79	-2.22	-3.07	/	10.8	-2.68	-0.03
H_2SO_4	0.	2.22	-0.45	-2.29	0.54	-0.02	0.
SO_4^{2-}	-2.02	/	3.52	2.29	/	-0.15	-3.64

*In the table TRT includes the contributions from transport and diffusion processes, CHEM stands for the gas-phase chemical production, AQUE accounts for the impacts of aqueous chemistry and cloud processes, G2P represent SO_4^{2-} production via the gas to particle processes, EMIS stands for emissions, and DRY and WET are for dry and wet deposition. Negative values indicate the mass of the species decreased by this processes.

Figure Captions

Figure 1. Average SO_2 emission rate (unit: mole/gridcell/sec) in the model domain. Also shown are the locations of four remote sites Sado, Happo, Oki and Hedo and two active volcanoes (Miyakejima and Sakurajima) in Japan.

Figure 2. Time series of measured (solid dots) and modeled (solid lines) SO_2 mixing ratios at four remote sites Sado, Happo, Oki and Hedo in Japan

Figure 3. The track of NOAA Ship Ronald H. Brown during ACE-Asia field campaign and time series of measured (solid dots) and modeled (solid lines) SO_2 and SO_4^{2-} mixing ratios. The numbers in plot A are Julian Day.

Figure 4. Horizontal distributions of SO_2 mixing ratios and wind vectors for the lowest model layer at 1200 JST from April 9 to 13.

Figure 5. Same as Figure 4 but for SO_4^{2-}(□g/m^3).

Figure 6. Horizontal distributions of vertically averaged HYPACT SO_2 concentration field at 1200JST from April 9 to 13.

Figure 7. Flight track (A) and time series of observed (solid dots) and modeled (open triangles) SO_2 mixing ratios (B) and SO_4^{2-} (C) for C130 flight RF 06 (April 11, 2001). The numbers in plot A are Japanese Standard Time (JST), and the flight altitude is show by a dashed line in plots B and C.

Figure 8. Same as Figure 7 but for flight RF 07 (April 12, 2001).

Figure 9. Same as Figure 7 but for flight RF 08 (April 13, 2001)

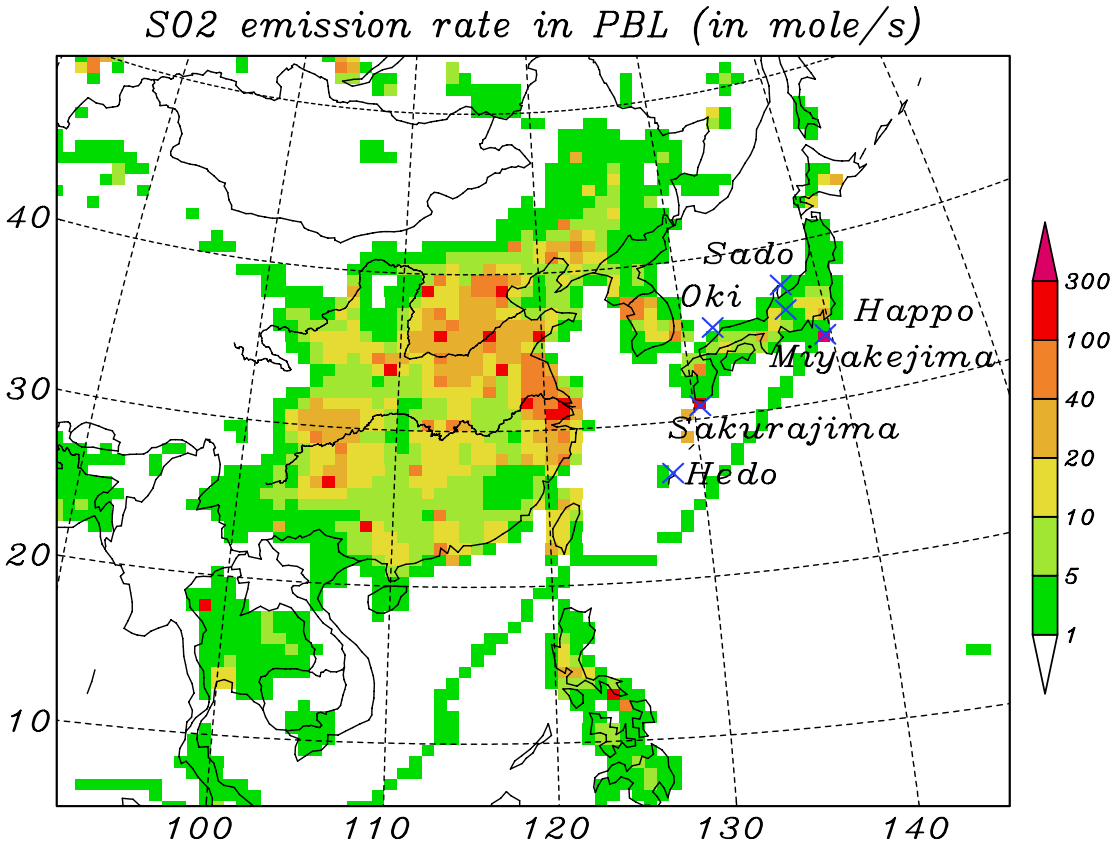

Figure 1. Average SO_2 emission rate (unit: mole/gridcell/sec) in the model domain. Also shown are the locations of four remote sites Sado, Happo, Oki and Hedo and two active volcanoes in Japan(Miyakejima and Sakurajima).

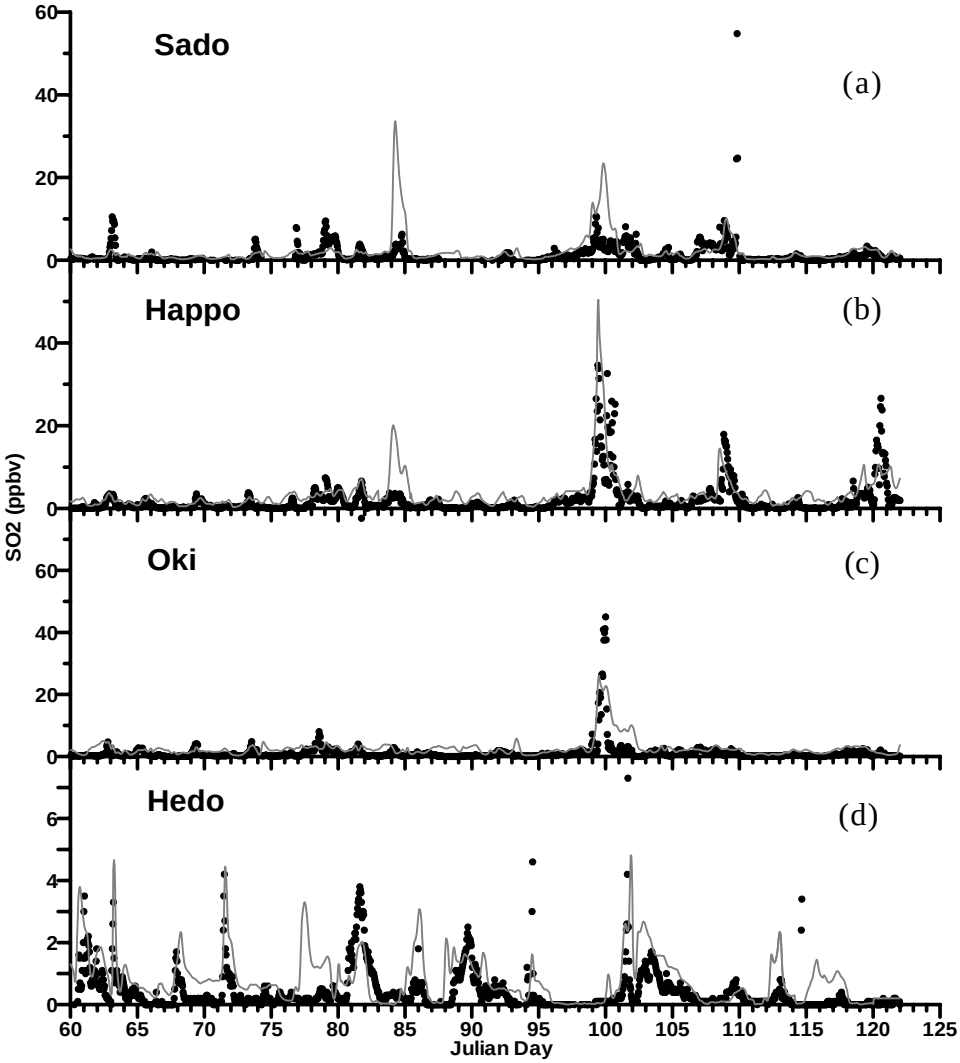

Figure 2. Time series of measured (solid dots) and modeled (solid lines) SO_2 mixing ratios at four remote sites Sado, Happo, Oki and Hedo in Japan.

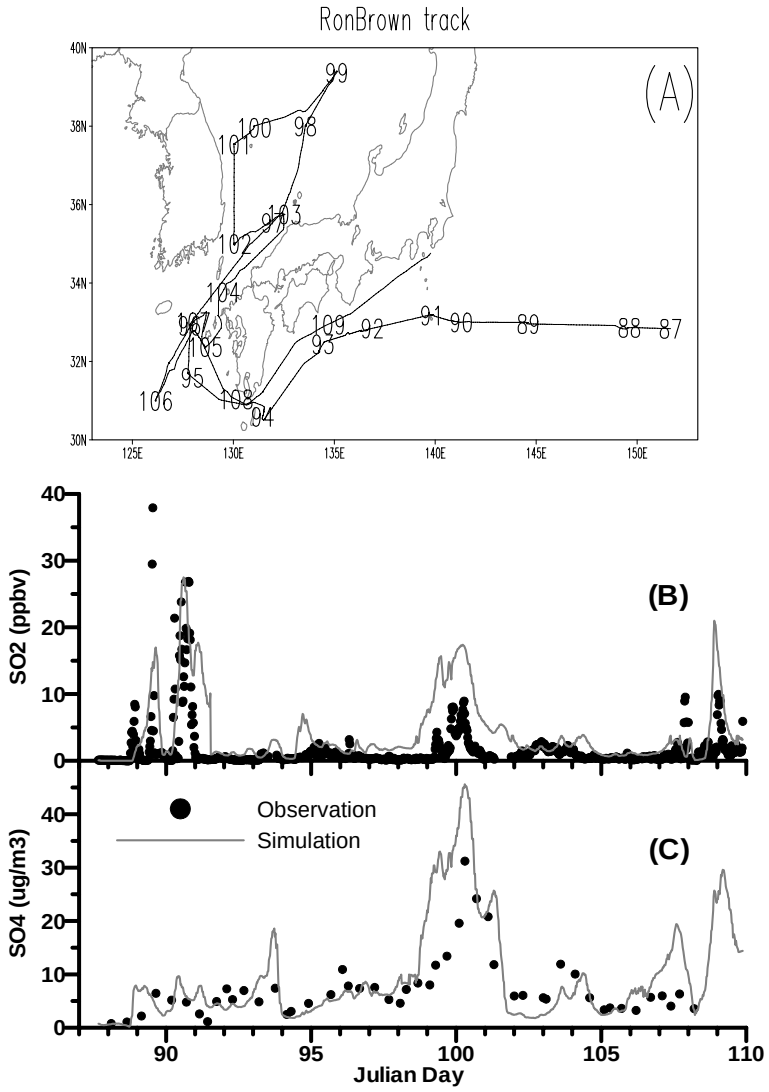

Figure 3. The track of NOAA Ship Ronald H. Brown during ACE-Asia field campaign and time series of measured (solid dots) and modeled (solid lines) SO_2 and SO_4^{2-} mixing ratios. The numbers in plot A are Julian Day.

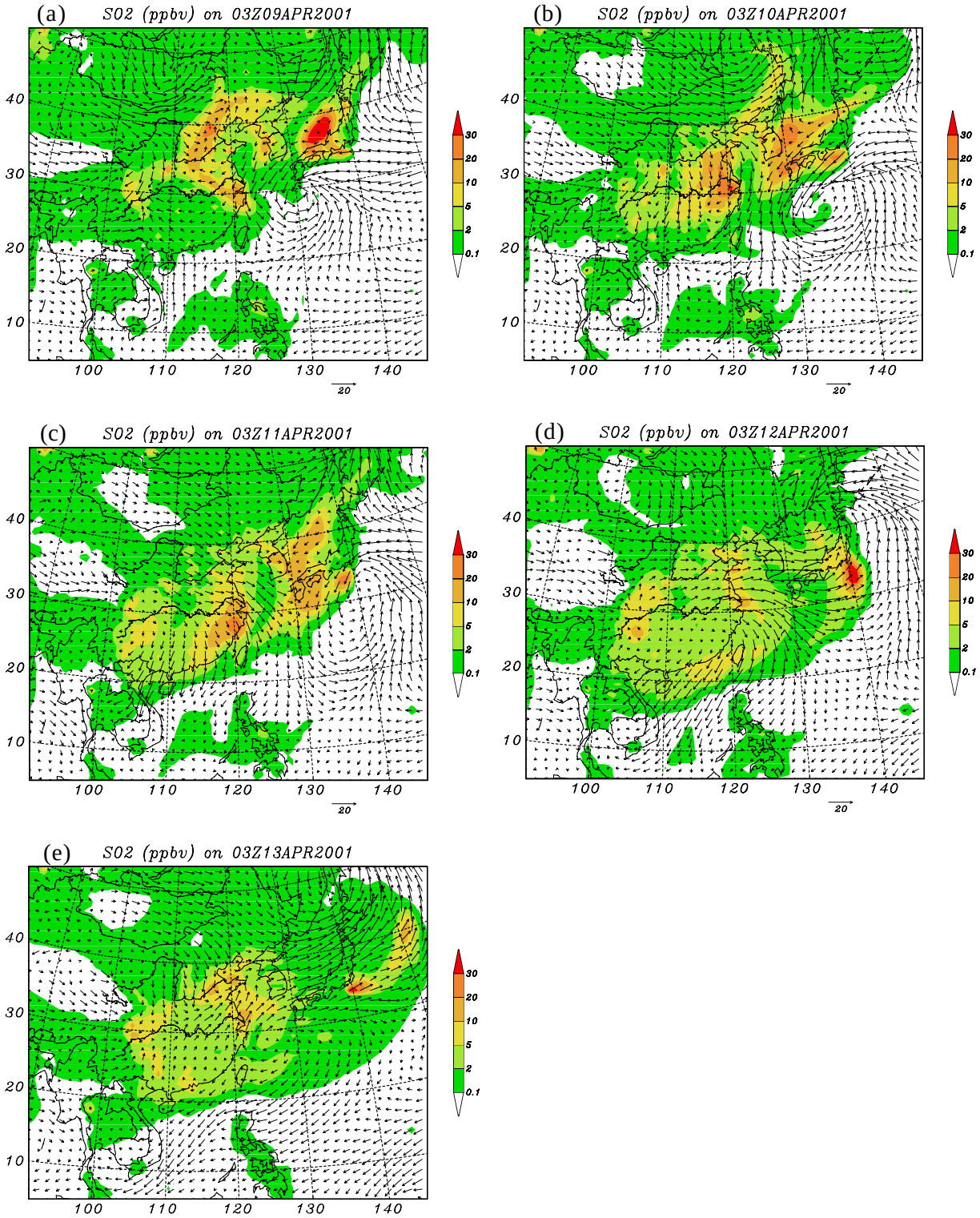

Figure 4. Horizontal distributions of SO_2 mixing ratios(ppbv) and wind vectors for the lowest model layer at 1200 JST on April 9 to 13.

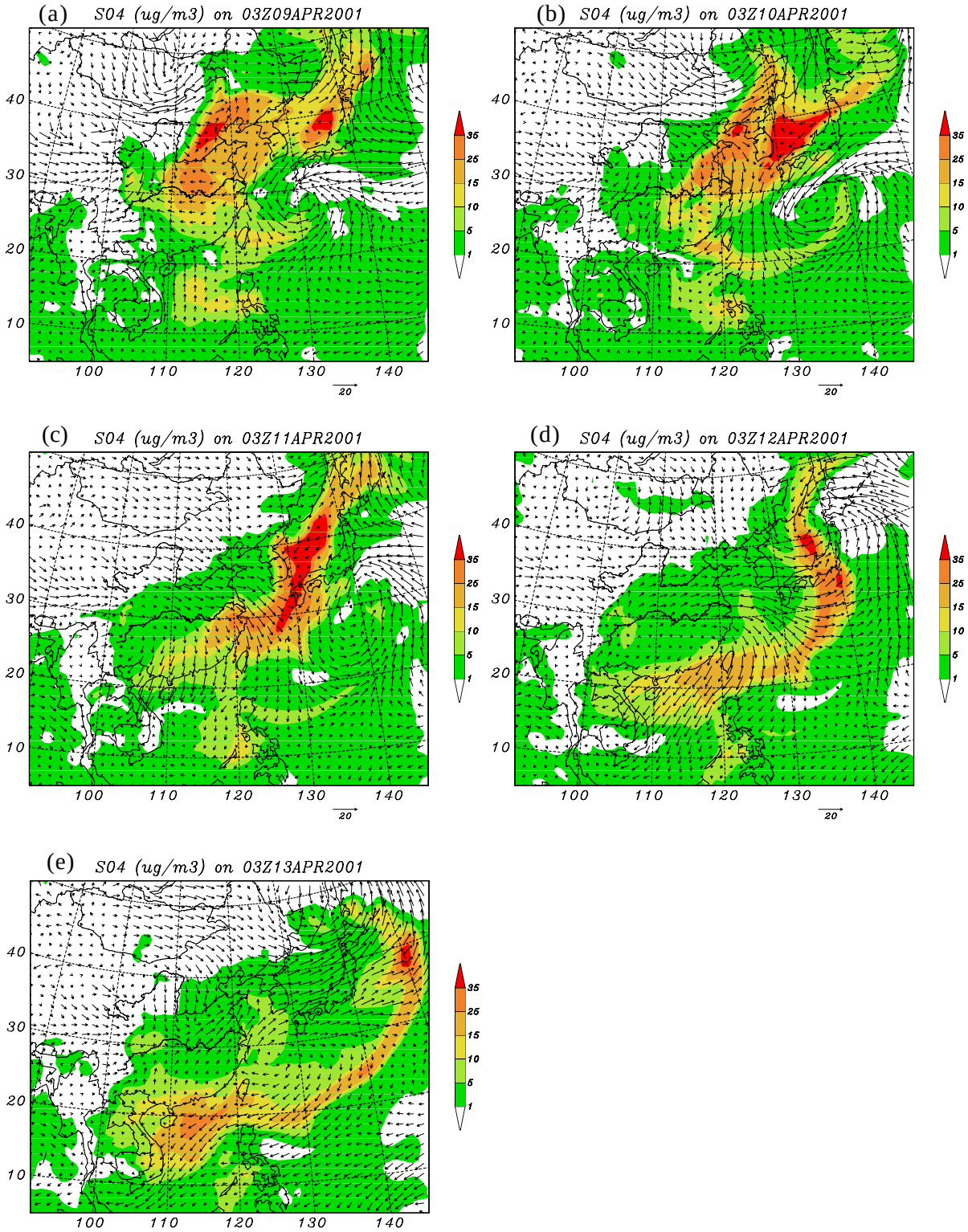

Figure 5. Same as Figure 4 but for SO_4^{2-}(μg/m^3).

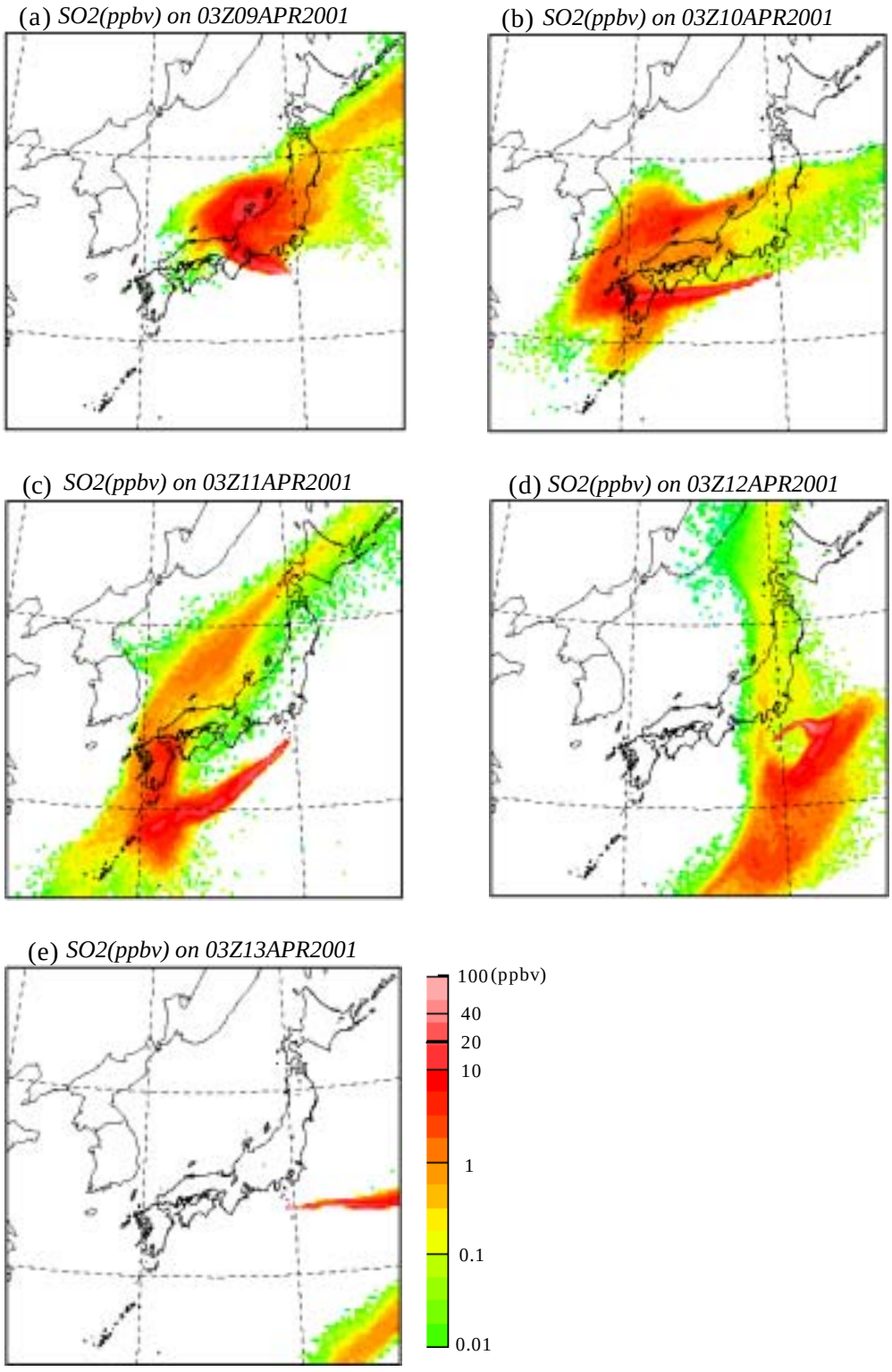

Figure 6　Horizontal distribution of vertically averaged HYPACT SO2 concentration fieldat 1200JST from April 9 to 13.

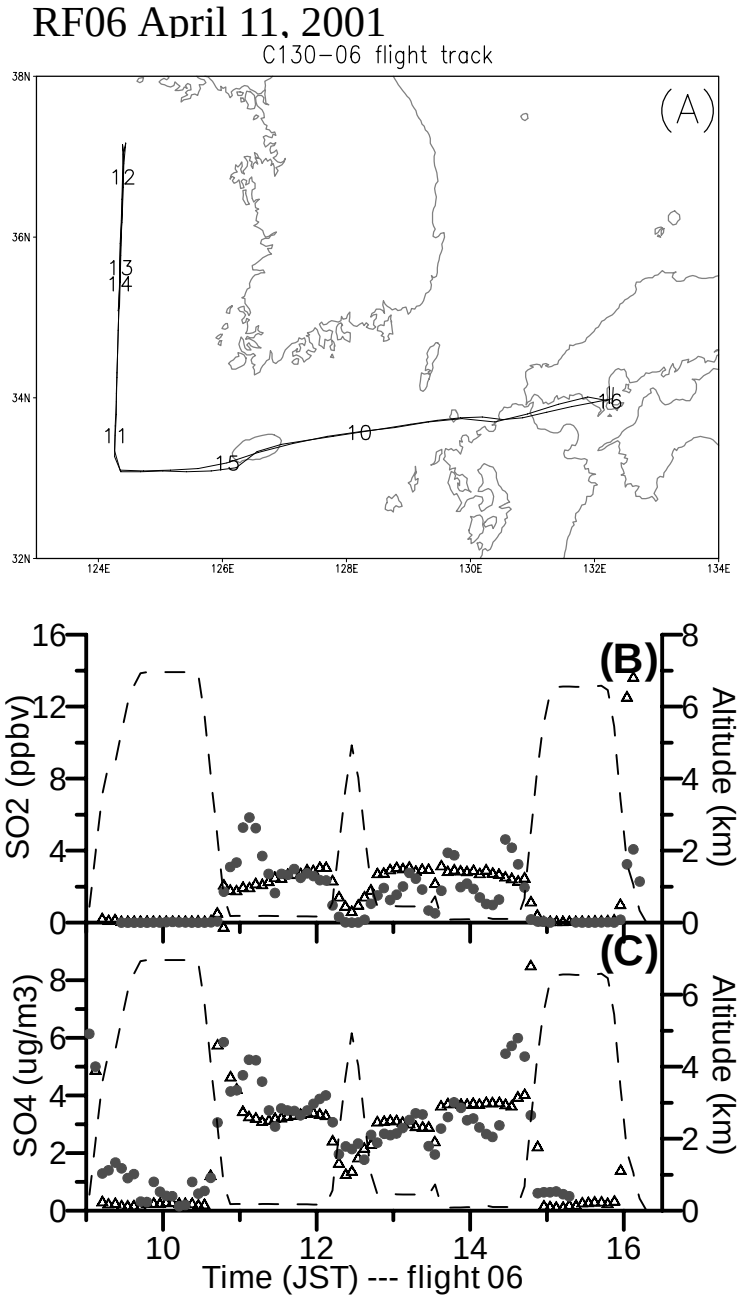

Figure 7. Flight track (A) and time series of observed (solid dots) and modeled (open triangles) SO_2 (B) and SO_4^{2-} mixing ratios (C) for C130 flight RF06. The numbers in plot A are Japanese Standard Time (JST), and the flight altitude is show by a dashed line in plots B and C.

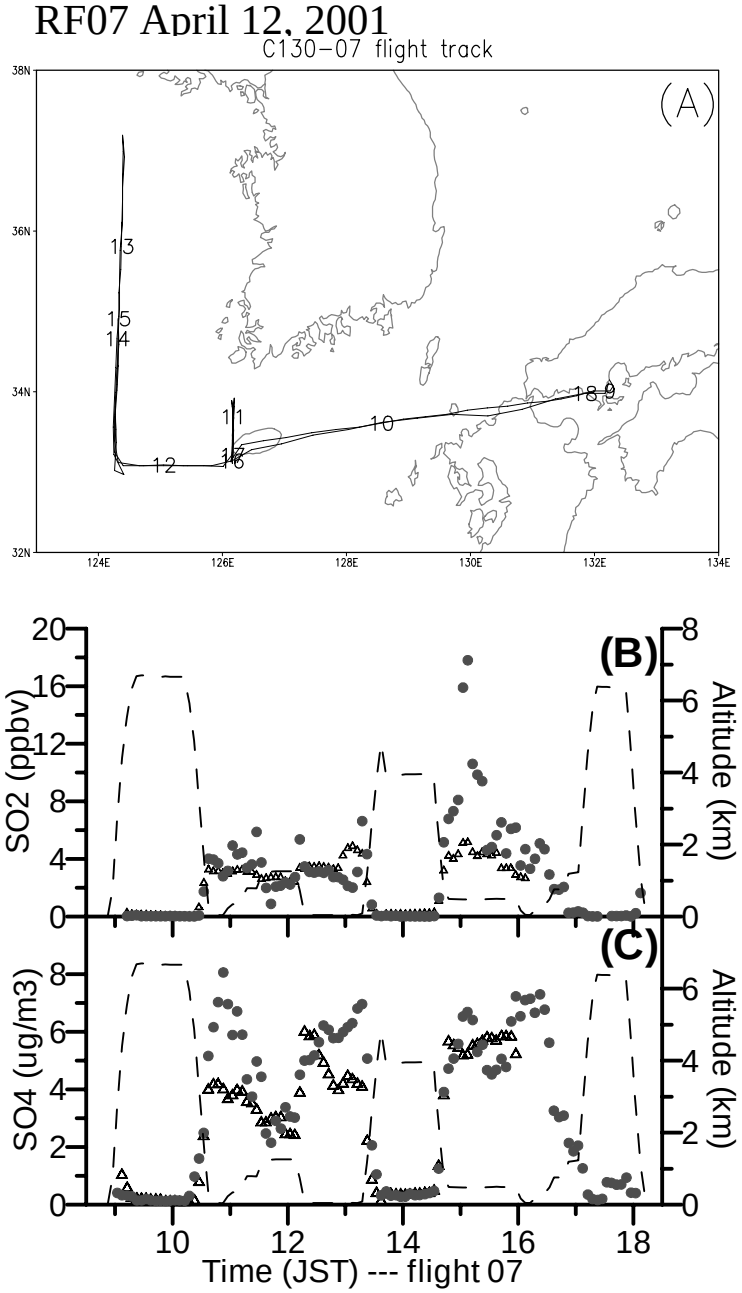

Figure 8. Same as Figure 7 but for flight RF07.

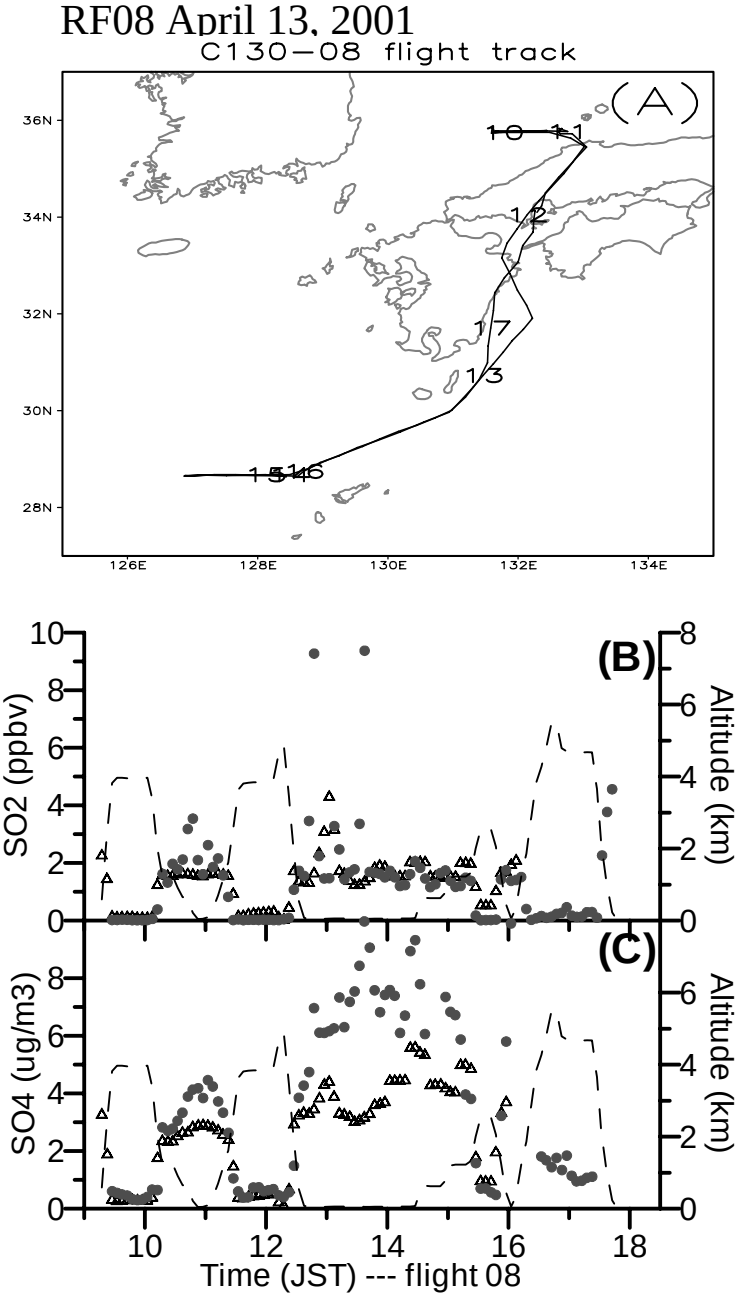

Figure 9. Same as Figure 7 but for flight RF08